

On the observed variability of the cross–polar cap potential

W. A. Bristow,¹ R. A. Greenwald,² S. G. Shepherd,³ and J. M. Hughes¹

Received 22 August 2003; revised 30 October 2003; accepted 5 December 2003; published 5 February 2004.

[1] A study of the cross–polar cap potential estimated by the HF Super Dual Auroral Radar Network (SuperDARN) during periods of steady interplanetary magnetic field (IMF) and solar wind velocity is presented. The potential estimates were examined as time series along with time series of the IMF and solar wind. In addition, the data were examined statistically to obtain a best fit linear expression for the potential as a function of the solar wind and IMF, which was used for comparison with observed potential values. It was found that the observed potential was significantly more variable than would have been predicted by the observed solar wind and IMF. The variability was found to be on the order of 20 kV, while the predicted variability would have been only 5 kV. Implications of these findings with regard to magnetospheric physics, ionospheric simulations, and space weather are discussed.

INDEX TERMS: 2784 Magnetospheric Physics: Solar wind/magnetosphere interactions; 2776 Magnetospheric Physics: Polar cap phenomena; 2736 Magnetospheric Physics: Magnetosphere/ionosphere interactions; 2740 Magnetospheric Physics: Magnetospheric configuration and dynamics; 2760 Magnetospheric Physics: Plasma convection

Citation: Bristow, W. A., R. A. Greenwald, S. G. Shepherd, and J. M. Hughes (2004), On the observed variability of the cross–polar cap potential, *J. Geophys. Res.*, 109, A02203, doi:10.1029/2003JA010206.

1. Introduction

[2] The cross–polar cap potential (PCP) parameterizes the degree to which solar wind energy is coupled into the Earth's magnetosphere. It is the difference in potential between the extrema of the high-latitude potential pattern, which usually are found at the centers of the two convection cells. It can be measured in the ionosphere by integrating the electric field along a line connecting the extrema. With the assumption that magnetic field lines are equipotentials, the PCP represents the instantaneous rate of flux transfer across the polar cap. Hence it is one of the best parameters available for describing the level of global-scale magnetospheric activity.

[3] A simple explanation for the source of the PCP is that for southward interplanetary magnetic field (IMF) conditions the polar cap field lines connect directly to the solar wind magnetic field and the solar wind electric field maps directly along the field lines [e.g., *Toffoletto and Hill*, 1989]. If one knew the amount of open flux threading the polar cap and the solar wind magnetic field strength and velocity, it would be a simple matter to calculate the PCP. This is attractive since the upstream IMF and solar wind plasma are monitored continuously, and it is possible to observe the location of the open-closed field line boundary, which provides an estimate of the flux threading the polar cap.

Unfortunately, this simple picture does not completely describe the situation. As magnetic field lines connected to the polar cap are swept antisunward with the solar wind, there are locations where the time derivative of the field is nonzero. Hence the field lines may not be equipotentials, and the electric fields may not map [e.g., *Lockwood et al.*, 1990].

[4] An alternative explanation for the source of the PCP is the combined effect of (1) the merging of magnetic flux on the dayside magnetopause and in the geomagnetic tail and (2) the so-called viscous interaction of the solar wind and the low-latitude boundary layer on the flanks of the magnetopause [*Cowley and Lockwood*, 1992; *Cowley*, 1982]. With such a source the PCP would be a function of the instantaneous value of the solar wind/IMF acting at the magnetopause and the history of the parameters that determine the merging rate in the magnetotail.

[5] Numerous studies have been undertaken to determine a relationship between observed solar wind/IMF conditions and the expected value of the cross-cap potential [e.g., *Heppner*, 1972; *Reiff et al.*, 1985; *Doyle and Burke*, 1983; *Reiff and Luhmann*, 1986; *Rich and Hairston*, 1994; *Boyle et al.*, 1997; *Weimer*, 2001]. These studies have been based on observations from polar-orbiting satellites as they traverse the high-latitude regions. Such observations require a period of time on the order of 20 min for the satellites to traverse the regions, and the time between observations may be on the order of about 100 min. Furthermore, a satellite may not observe the complete cross-cap potential on any given orbit, since it may not reach a sufficiently high latitude. The combination of these factors leads to a large uncertainty in the observations.

[6] Despite the uncertainty, sufficient data have been collected to determine a functional dependence between

¹Geophysical Institute, University of Alaska Fairbanks, Fairbanks, Alaska, USA.

²Applied Physics Laboratory, Johns Hopkins University, Laurel, Maryland, USA.

³Thayer School of Engineering, Dartmouth College, Hanover, New Hampshire, USA.

solar wind/IMF parameters and the expected potential. The best fit lines are the sum of a baseline potential and a function of the solar wind velocity, the magnitude of the IMF, and the IMF clock angle. The baseline potential is assumed to be due to the solar wind viscous interaction. *Reiff and Luhmann* [1986] presented observations with a correlation coefficient of greater than 0.9 for one such line. Their data, however, show a large scatter about the line. For given values of the solar wind/IMF parameters the value of the potential showed a spread of as much as 40 kV.

[7] The observed variation could be attributed to the uncertainty in the potential measurement discussed above or to uncertainty in the solar wind/IMF observations. The sources of uncertainty in the solar wind/IMF observations relate to the timing and the scale size of solar wind and IMF structures [e.g., *Crooker et al.*, 1982; *Burke et al.*, 1999]. Because the observations come from an upstream monitor that may be some distance from the magnetopause or from the Earth-Sun line, it is often difficult to determine the time at which the observed solar wind/IMF was effective at Earth or even if the observed structure is the same as that in effect at the magnetopause. In addition, it is likely that the solar wind/IMF often changed during the 20-min periods that were required to complete each potential observation.

[8] With such large measurement uncertainties it is not possible to determine the inherent variability of the potential. That is, it is not known whether a given set of solar wind parameters will produce a certain value of the potential or rather if a range of values could be expected. Since the potential may depend not only on the instantaneous value of the solar wind/IMF parameters but on their history as well, significant variations of the potential would be expected about a line determined as a function of the instantaneous parameter values.

[9] *Cowley and Lockwood* [1992] noted the large variability of the potential when plotted versus the solar wind electric field (vB_z) and attributed it to such a source. They noted that the implicit assumption in plotting the potential versus some function of the instantaneous solar wind/IMF values is that the convection pattern becomes established immediately when the values take effect at the magnetopause. They contended that there should be an initial response to the solar wind/IMF as reconnection commences at the subsolar point and a second response that is delayed by some 30 min or so when reconnection commences in the tail. In a simple two-component response model they showed an expected response to a step change of the IMF from steadily northward to steadily southward. The PCP was expected to increase rapidly to a level and remain steady until a later time when it would double and then remain steady again. *Cowley and Lockwood* presented a similar expected two-step response for convection decay when the IMF switches northward. More recent studies of the time for convection to respond to changes in the IMF show rapid response at all local times and do not lead to the expectation of a two-step response [*Ruohoniemi and Greenwald*, 1998; *Greenwald et al.*, 1999; *Shepherd et al.*, 1999].

[10] In this paper, observations of the variability of the PCP are examined. In the examination, two steps were taken to reduce the observational uncertainties and to isolate the variability. First, the Super Dual Auroral Radar Network (SuperDARN) [*Greenwald et al.*, 1995] was used to deter-

mine the potential. Second, periods were chosen when the IMF remained relatively constant for periods of about 2 hours or longer. The main advantage of using SuperDARN observations is that they can provide an estimate of the potential based on data obtained over about 2 min. While significant potential variations over short time periods are possible, their effects are minimized by using such a fine time resolution. Another advantage of the SuperDARN observations is that they provide a time series rather than a snapshot every 100 min.

[11] Examining periods when the IMF was relatively steady minimized the uncertainty about the conditions in effect at the time of the potential observations. Also, by examining time series of potential observations for steady IMF conditions, it was possible to investigate the degree of variability that is due to internal magnetospheric sources. Finally, it was possible to determine if there was evidence of a two-step response of the convection.

2. Data Presentation

[12] Periods were chosen for examination on the basis of observations from the Advanced Composition Explorer (ACE) spacecraft. The criterion for selection was that the three IMF components remained within certain ranges for periods of greater than 2 hours. The motivation for restricting the study to such periods was, as discussed in section 1, the uncertainty in the timing of solar wind features observed at an upstream monitor becoming effective at Earth. By using long periods of steady IMF, this uncertainty is minimized. In addition, it was expected that the uncertainty due to the scale size of solar wind features would also be reduced. The IMF ranges used were $-10 \text{ nT} < \text{IMF } B_x < 10 \text{ nT}$, $-4 \text{ nT} < \text{IMF } B_y < 4 \text{ nT}$, and $-10 \text{ nT} < B_z < -2 \text{ nT}$. These ranges were chosen with the expectation that the convection patterns were similar for all of the intervals yet were not so limiting that the number of intervals would be small. While the ranges appear large and would allow for significant variation, the data show that the IMF was generally steady during the individual intervals, as will be illustrated in Figures 3 and 4. Data from the full year of 2001 were examined for intervals meeting these criteria. In the year's data, there were 43 intervals for a total of 159 hours of observations. Of those 43 intervals, 37 had sufficient radar observations to form estimates of the PCP. Figure 1 shows the distribution of the three components of the IMF from the 37 intervals. The z component had an average value of -5.37 nT with a standard deviation of 1.68 nT , while the y component had an average value of -0.047 nT and a standard deviation of about 1.78 nT . This shows that the majority of the time, the z component was significantly southward and was greater in magnitude than the y component. It is interesting to note that the x component observations appear bimodal, with a broad distribution centered on zero and a second narrow distribution centered on about -1.3 nT . This narrow distribution may indicate that the steady conditions are more likely to occur when the spacecraft is some distance from the ecliptic plane. With the selected predominantly southward IMF conditions the expected convection would be a simple two-cell pattern. Additionally, these conditions were conducive to this study since the expected convection patterns usually produce

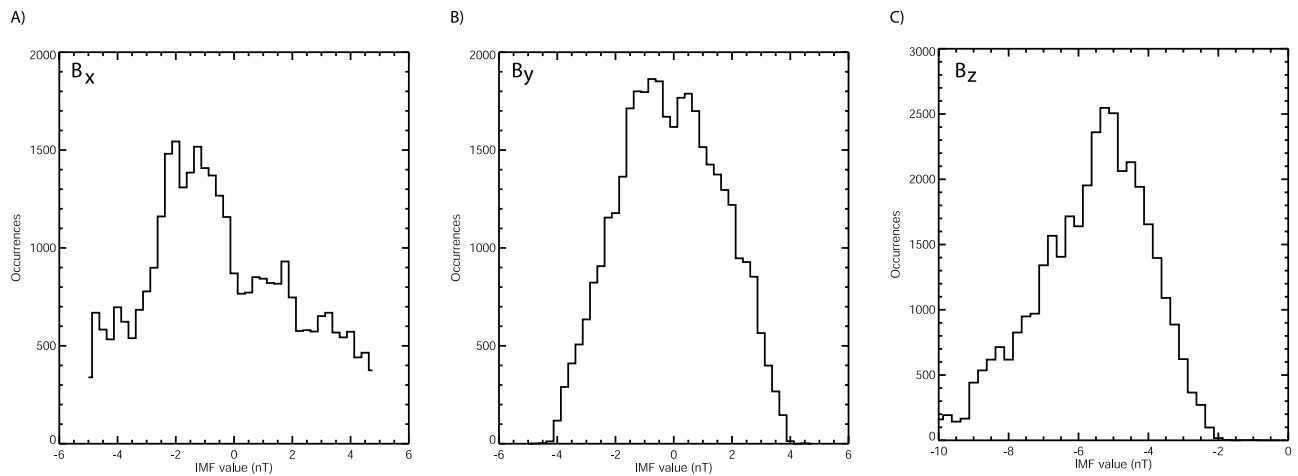


Figure 1. Distribution of 16-s interplanetary magnetic field (IMF) observations from the study periods: (a) x component, (b) y component, and (c) z component.

relatively abundant plasma irregularities in the latitude range best observed by the radars.

[13] Estimating the PCP from the radar data requires a sufficient number of plasma drift velocity observations to form the high-latitude convection pattern. The technique for estimating the high-latitude convection pattern by combining observations from the SuperDARN radars was described by *Ruohoniemi and Baker* [1998]. Briefly, the technique uses line-of-sight velocity data from all of the radars in the network to constrain a spherical harmonic expansion of the high-latitude ionospheric potential. The PCP is a direct product of the fit. Figure 2 shows a sample convection pattern from the interval 1340–1342 UT on 15 January 2001. For this pattern, and all succeeding patterns, the IMF condition in effect was determined from observations by the ACE satellite, assuming the transit time from ACE to Earth was about 50 min. The conditions in effect during the interval shown in Figure 2 were B_z southward with small positive B_y , as is indicated by the axis in the upper right-hand corner of the plot. The plot shows a two-cell pattern with roughly equally sized evening and morning cells. The vectors on the plot indicate the region of data coverage. In the regions where no data vectors are plotted, no radar scatter was received, and the expansion was constrained by a statistical model of the convection pattern. The total PCP is indicated in the lower left-hand corner of the plot. In this case the potential was 56 kV. Because of the amount of data coverage the potential was well determined by the fitting procedure.

[14] There is always some uncertainty in the PCP measurement because of incomplete coverage and uncertainty of the individual measurements. This uncertainty can cause an apparent variation of the potential when there was no actual variation. For example, a reorientation of the potential pattern could move a potential extremum into or out of the field of view of the radars. Since the potential pattern estimate is a fit constrained by observations, the total potential drop is certain only when the observations cover the region from the minimum to the maximum or from zero to the maximum and from zero to the minimum. Any reorientation of the pattern that moves the maximum, the minimum, or zero away from or closer to the field of

view of the radars would appear as a change of the potential. It is also possible that a change in the number of data points within the radar fields of view could give the appearance of a change in the potential. The reason for the apparent variation is the same as that for a reorientation of the pattern; that is, an increase or decrease in the number of observations could move the extrema into or out of the regions included in the fit. To eliminate this source of uncertainty, one might attempt to form a series of potential estimates by using only those regions where data coverage remains constant throughout the interval. Unfortunately, however, this tactic could result in underestimating the amount of variability. The reason for this is

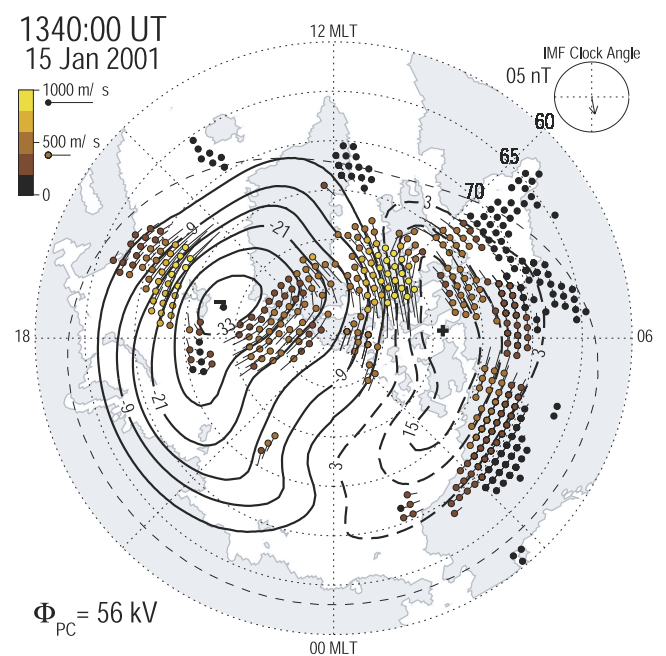


Figure 2. Convection pattern observed by the Super Dual Auroral Radar Network (SuperDARN) during the interval 1340–1342 UT on 15 January 2001.

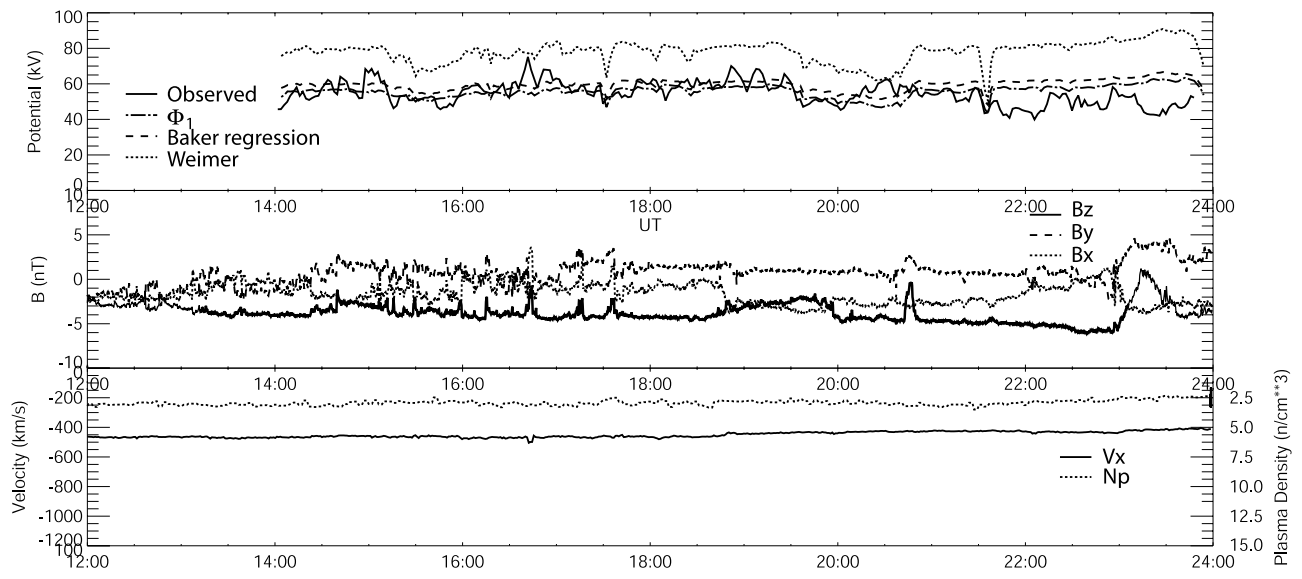


Figure 3. Observed cross-polar cap potential, IMF, and solar wind velocity and density from 1200 to 2359 UT on 11 January 2001. Estimates of the potential based on solar wind and IMF are plotted over the observed potential. The IMF and solar wind observations are plotted at the time observed and are not shifted to the expected time of impact at the magnetopause.

that the sudden appearance or disappearance of scatter within the radar field of view can indicate changes in plasma velocity, which controls the formation and decay of the irregularities from which the radar signals scatter. Furthermore, while a reorientation of the flow pattern can cause an apparent change in the potential even if one was not present, that reorientation represents a change to the convection that would not be predicted by the observed solar wind conditions.

[15] In addition, incomplete data coverage results in uncertainty in the absolute magnitude of the potential. To minimize this uncertainty, periods were selected on the basis of having a sufficient number of observations so that the potential was primarily controlled by the observations and the influence of the statistical model was minimal. Furthermore, the absolute magnitude of the potential was of less concern than was its variation, which was controlled entirely by the observations since the IMF values used to select the statistical model were steady for each period. As will be illustrated by examples, the observations show a significant amount of variability.

[16] As was discussed in section 1, SuperDARN is capable of producing an estimate of the potential pattern every minute or 2 min, depending on the experiment mode. By doing so for periods of relatively steady IMF, it was possible to obtain time series of PCP values for approximately fixed IMF values. Figure 3 shows the PCP, IMF, and solar wind velocity and density for one such interval. The selected interval, 11 January 2001, was the first interval of 2001 that met the selection criterion. The IMF met the criterion starting at about 1300 UT. The field remained steady at around 5 nT southward from about 1300 UT to about 2300 UT. While there are numerous short-duration fluctuations of a few nanoteslas during the interval, the average value of the field remains steady, and there are

significant intervals when the fluctuation level is less than 1 nT. Superposed on the trace of the estimated charge and current probe (CCP) are three lines showing the value of CCP that would be predicted from the observed solar wind and IMF. Two of the predictions are based on the following formulae:

$$\Phi_1 = 42.956 + 9.08VB \sin^3(\theta/2)$$

$$\Phi_2 = 36.900 + 9.7VB_z + 3.1|VB_y|,$$

where B is the magnitude of the IMF component in the y - z plane and V is the solar wind x velocity. The first formula was determined by linear least squares fit to the data from this study. The second was determined by Baker [2002] by carrying out a multiparameter regression on an independent sample of SuperDARN potential measurements. The potential predictions were calculated from 2-min averages of the IMF and solar wind velocity with a 50-min lag from the time of observation. The techniques used to obtain these formulae are described below and are similar to those used in previous studies of the solar wind dependence of the polar cap potential. Using formulae determined from SuperDARN data should eliminate instrumental biases that would result from using another source. Both lines show good agreement for the mean value for much of the interval. They do not, however, reproduce the large fluctuations of the potential.

[17] The third model potential estimate was determined using a statistical model of the high-latitude potential pattern [Weimer, 2001]. These potential estimates were also calculated from 2-min averages of the IMF lagged by 50 min. Two features are apparent from this line. First, the potential prediction is significantly higher than the observed value. In this interval, and in most of the intervals included in this study, the model potential was on the order

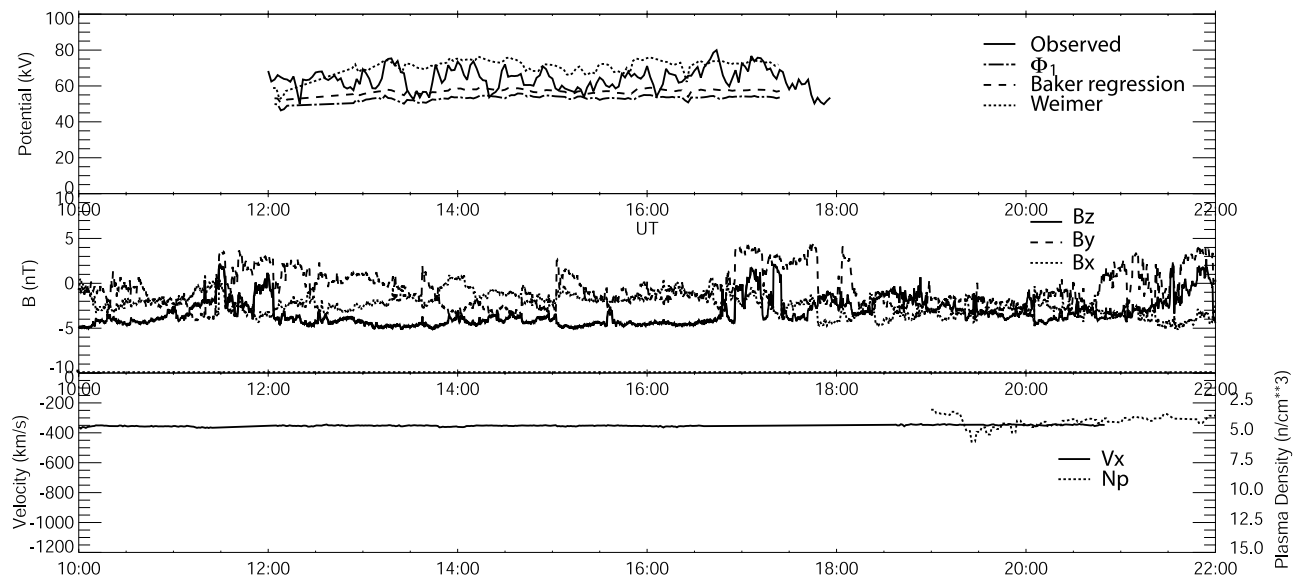


Figure 4. Observed cross-polar cap potential, IMF, and solar wind velocity and density from 1000 to 2200 UT on 15 January 2001. Estimates of the potential based on solar wind and IMF are plotted over the observed potential. The IMF and solar wind observations are plotted at the time observed and are not shifted to the expected time of impact at the magnetopause.

of 20 kV higher than was observed, or about four thirds of the observed value. Second, the model exhibits a higher level of variability than the regression formulae derived from the SuperDARN observations. The two features are in fact related in that the higher potential value represents a stronger dependence on the value of IMF B_z . This implies that a larger fluctuation of the potential will result from a fluctuation of B_z than would be predicted by the SuperDARN regression formulae. The amplitude of the fluctuations predicted by the model in response to the observed IMF fluctuations was on the same order as the observed potential fluctuations. It should be noted, however, that in intervals when the IMF is steady, the observed potential maintained about the same level of fluctuation, while the model prediction remained steady.

[18] During the interval 1308–1330 UT on 15 January 2001 the average IMF B_z value was about -5 nT with a deviation of 0.18 nT. This was another interval when the IMF, solar wind velocity, and solar wind density were all quite steady. The only significant deviations were in the IMF, and they were short-lived spikes of a few nanoteslas. In this case, as illustrated in Figure 4, the predicted mean value of the potential was significantly different from the observed value. In addition, the observed potential again showed significantly larger variation than was predicted. The potential had an average value of about 62 kV and a peak-to-peak variation of about 20 kV, while the predicted mean value was about 55 kV with a variation of less than 5 kV. While the difference between the observed mean and the predicted mean is not a focus of this study, it is worth noting that during most of the intervals examined the observed and predicted means were similar. There were, however, a few intervals, such as the 15 January period, during which the means were different.

[19] Examination of the convection patterns for the interval showed that the variations of the potential were due to

localized flow enhancements at various locations around the high-latitude region. Some of the enhancements appeared to originate near the noon and midnight regions, though this was not always the case. Often, short-lived flow enhancements appeared to originate at local times away from noon and midnight. To illustrate this, Figure 5 shows a sequence of six convection patterns taken from the 20-min interval 1308–1328 UT, showing a flow enhancement that appears to be localized to the region near 0200 magnetic local time (MLT). The initial pattern, 1308 UT, shows a cross-cap potential of about 58 kV, which increased to 75 kV by 1316 UT and decreased back to 58 kV by 1328 UT. The IMF conditions, illustrated by the clock angle plot in the upper right corner of each frame, were steadily southward at about 5 nT. Over the period the region of flow near 0200 MLT between 70° and 75° magnetic latitude increased from about 500 m/s to over 800 m/s and decreased back to 500 m/s. Data coverage remained fairly constant over the period as did flow velocities in other areas, which indicates that the potential enhancement was due to the localized flow increase. Furthermore, on the basis of the location of the increase it can be concluded that the potential enhancement was due to internal magnetospheric variability rather than variability of the external driver.

[20] Another point of interest is illustrated by comparing Figures 3 and 4. The two cases are strikingly similar in all respects but one. In both cases the IMF remained steady for an interval of more than 2 hours and had an average value of about 5 nT. The solar wind velocity appeared steady throughout the periods and had similar magnitudes. The resulting potential showed a steady mean value throughout both intervals with variations of about 20 kV. The difference between the two cases is that the mean value of the potential in the 15 January case was 10–15 kV higher than in the 11 January case and was underestimated by the regression formulae. There is nothing in the solar wind or IMF that

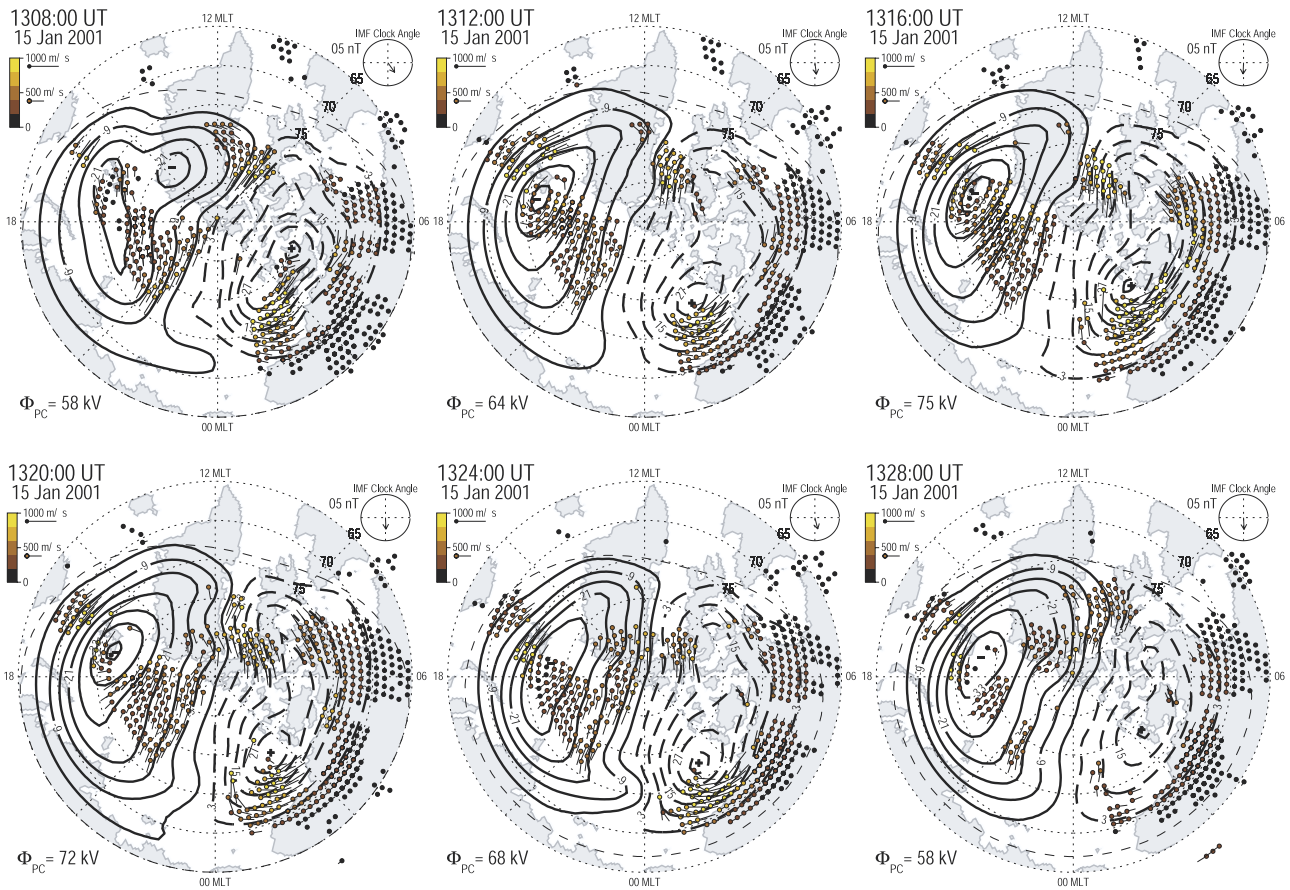


Figure 5. Sequence of convection patterns observed by SuperDARN covering the interval 1308–1328 UT on 15 January 2001.

would lead one to expect such a difference in the potential. In the majority of the intervals examined under this study, the mean values were estimated quite well by the regression formulae. There were, however, a few cases where there were differences similar to that illustrated on 15 January, for which there was no clear indication of a cause. It is possible that the differences were due to differences in the amount of data coverage between the two intervals. The 11 January interval had less coverage, and the potential estimate was more strongly influenced by the statistical model. In addition, however, the observed flow velocities were lower on 11 January than on 15 January. The spatial mean observed flow velocity on 11 January ranged between 400 m/s and 500 m/s, while on 15 January it ranged between 500 m/s and 600 m/s. This indicates that the observed difference of the potential represents a real difference in the average potential.

[21] PCP data from all of the study intervals were combined in scatterplots versus various functions of the solar wind, and IMF parameters and correlation coefficients were calculated for each function. The correlation coefficients and the amount of scatter about lines of best fit were similar for each of the functions examined. Figure 6 shows the potential plotted versus the product of the solar wind x component velocity, the magnetic field magnitude, and the cube of the sine of the solar wind clock angle. The points in Figure 6 represent the potential values determined for each 2-min interval for

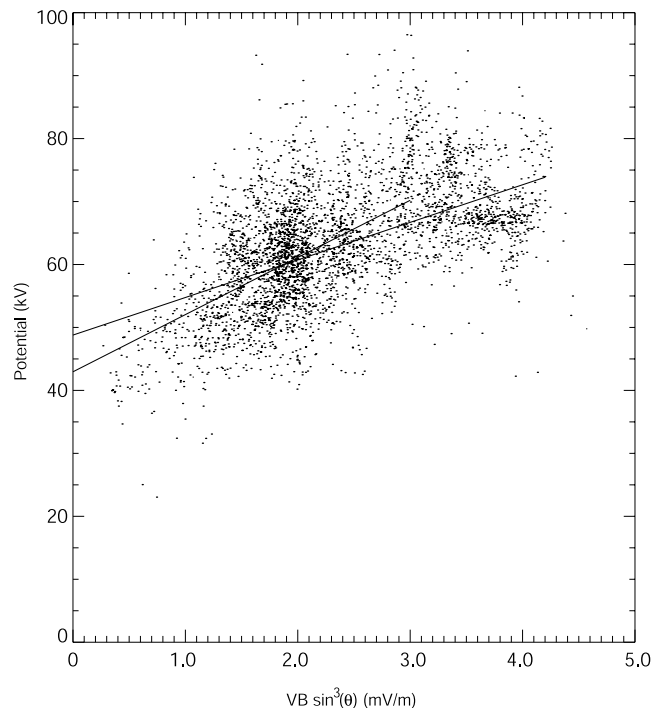


Figure 6. Scatterplot of observed cross-polar cap potential versus solar wind electric field. The superimposed lines indicate the best fits for all data and for electric field values of less than 3 mV/m.

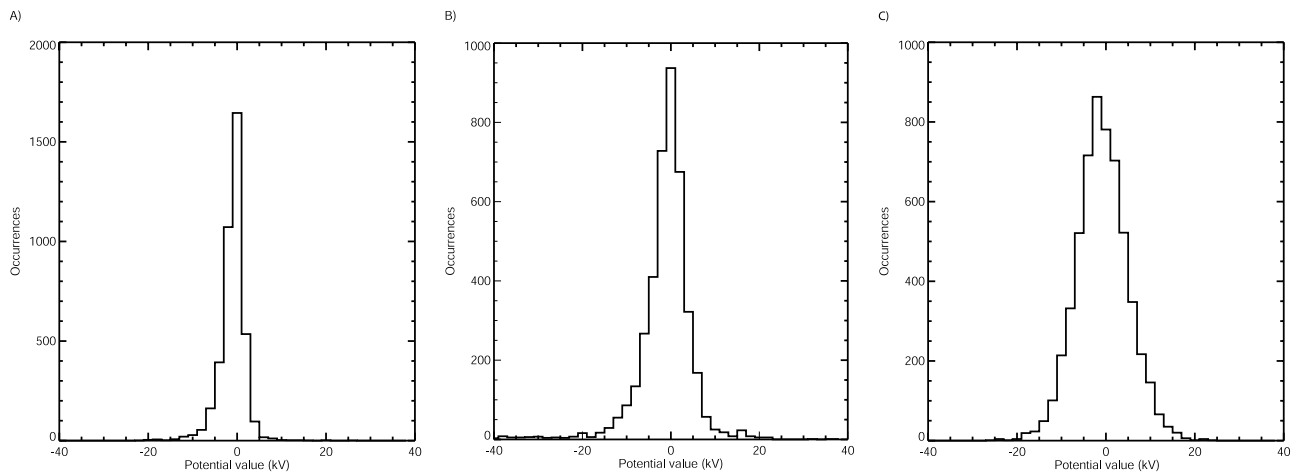


Figure 7. Distribution of detrended potentials estimated from (a) the solar wind and IMF using the Baker [2002] regression, (b) Weimer [2001] potential model, and (c) observed convection.

which both solar wind and IMF measurements were available. The best fit line from this plot determined the potential Φ_1 used in Figures 3 and 4. The plot is similar in form to those produced by other authors [e.g., Reiff and Luhmann, 1986] as described above, illustrating a similar amount of scatter about the best fit line. The data show a clear trend as illustrated by the two fitted lines, which were calculated by fitting different portions of the data. The line with the lesser slope was calculated using all of the data, while the steeper line calculation excluded data for solar wind electric fields of greater than 3.0 mV/m. The motivation for fitting over a limited portion of the data is that some studies [e.g., Shepherd *et al.*, 2003] have shown that there may be a saturation of the potential for large values of the solar wind electric field. The difference in slope for the two fits indicates this saturation. While this study is not concerned with the saturation, it was necessary to choose one of the fitted lines to estimate the potential from the observed solar wind and IMF for each interval. Since 75% of the data from this study came from intervals with solar wind electric field of less than 3.0 mV/m, the equation for Φ_1 was used to estimate the potential in the time series plots.

[22] To determine the variability of the potential that would not have been predicted by the observed variability of the solar wind and IMF, distributions of the potential and the potential predicted from the regression formula were examined. Since it was observed that at times the average value of the potential for the study periods differed from the predicted value, the data and the predictions were detrended independently, and distributions of the detrended data were examined. The detrending was carried out by subtracting a second-order polynomial fit from each 2-hour period of data and predicted potential. Figure 7 shows the distributions of detrended model predictions of the potential and the detrended observed potential. Figure 7a, which shows the potential predicted by the SuperDARN regression formulae, is narrow, showing a variability of less than 5 kV at half of the peak of the distribution. This illustrates the steadiness of the IMF and solar wind

during the study intervals. Figure 7b shows the distribution of potential predicted by the statistical potential model. This distribution is nearly twice as broad as that in Figure 7a, illustrating the higher predicted level of fluctuation. Figure 7c, which shows the distribution of observed potentials, is relatively broad, with a width of about 20 kV at half maximum. Hence the observed variability is about twice that predicted by the statistical model and about four times as large as that predicted by a linear regression formula. Another feature to note is that the distribution of predicted potentials is skewed somewhat about 0, while the observed distribution appears symmetric.

3. Discussion

[23] The observations presented here clearly indicate that the cross-polar cap potential exhibits a significant level of variability that would not be predicted from observations of its primary driver, the solar wind electric field. Furthermore, they imply that a certain set of solar wind/IMF parameters will not necessarily produce a certain value of the cross-cap potential. Rather, a certain mean value would be expected, with some range of fluctuation being likely. While these implications are not unexpected, they are worthy of study and should be quantified. They have implications regarding the internal workings of the magnetosphere and have practical implications regarding studies of magnetospheric physics, ionospheric physics, and space weather.

[24] As discussed in section 1, the cross-polar cap potential is one of the fundamental parameters that characterizes the state of the magnetosphere and the interaction between the solar wind/IMF and the magnetosphere. It is used as a benchmark for magnetospheric simulations, and its equivalent is used as a driver for global-scale ionospheric and thermospheric simulations. If it is assumed that the PCP arises from the combined effects of dayside and nightside merging, the variability indicates the level to which the merging process is bursty or patchy. Furthermore, since the potential fluctuations appear at times to arise from flow increases located away

from either noon or midnight, they indicate that other internal mechanisms influence the potential. This would be expected since phenomena such as bursty bulk flows and substorm-associated flows should influence the PCP. The results presented here provide some insight into the level at which these phenomena can influence the potential. The width of the distribution of observed potential was about 20 kV and appeared to be relatively independent of the mean value of the potential. Since the observed mean potentials ranged mainly between 40 and 80 kV, the fluctuation ranged from 25% to near 50%.

[25] Ionospheric simulation studies have demonstrated that variability of the electric field in the ionosphere on small spatial and temporal scales can significantly elevate the amount of Joule heating predicted by the simulations [Codrescu *et al.*, 1995, 2000]. Variability of the PCP, as an integral measure, does not provide information on spatial scale. It would, however, affect the results of simulations and should be accounted for. The PCP influences ionospheric and thermospheric simulations through the convection pattern. In most simulations the observed IMF is used to select a convection pattern from a statistical model. The models provide a fixed potential pattern for a certain IMF value. For steady IMF conditions, there is no variability in the simulation driver. Variability of the PCP would be reflected in the strength of the convection and in the locations of the potential maxima and minima. Ideally, simulations should use measured convection patterns whenever possible. When measured convection is not available, such as when simulations are used in a predictive mode, it should be possible to parameterize the PCP variability for use as a driver.

[26] In the majority of the intervals examined in this study, the mean value of the potential was characterized well by the value estimated from the solar wind and IMF. The regression formula used to estimate the potential are not necessarily the same as would be obtained from a statistical convection model, but as was discussed, several functions of the solar wind and IMF were examined, and each produced similar results. Hence it is likely that statistical convection models reasonably reproduce the mean value of the potential for given IMF and solar wind conditions.

[27] A recent study of high-latitude ground magnetometer perturbations [Weigel *et al.*, 2003] showed similar results to those obtained here. In that study a neural network driven with solar wind and the IMF was used to estimate the magnetometer perturbations and their time derivatives as a function of local time. For some local times the neural network predicted as much as 70% of the variance in the magnetometer perturbations, while at some other local times, only about 10% of the variance was predicted. As an integral measure that incorporates all local times, the cross-polar cap potential would be expected to show a level of predictability that is somewhere between these two extremes.

[28] The implication of the observed PCP variability for space weather is relatively straightforward. If the IMF and solar wind observed at an upstream monitor are used to predict the PCP or some other integrated measure of

magnetospheric activity, the prediction should be stated as a probability that the PCP will lie within some range. The consistency of the observed mean values and variability indicate that such predictions would be fairly robust.

[29] This study addressed the variability for periods with steady solar wind electric field conditions, which represents only a fraction of the time during a year. For the year 2001, only 159 hours met the criteria used for selection. Further study is needed to characterize the variability under non-steady conditions. This is a more difficult task that will be addressed elsewhere.

[30] **Acknowledgments.** This work was supported by National Science Foundation grant OPP99-81866 from the Arctic Natural Sciences program of the Office of Polar Programs.

[31] Arthur Richmond thanks Frederick J. Rich and another reviewer for their assistance in evaluating this paper.

References

- Baker, K. B. (2002), Fit ACF, paper presented at the annual SuperDARN project meeting, Natl. Sci. Found., Valdez, Alaska, May.
- Boyle, C. B., P. H. Reiff, and M. R. Hairston (1997), Empirical polar cap potentials, *J. Geophys. Res.*, *102*, 111–125.
- Burke, W. J., D. R. Weimer, and N. C. Maynard (1999), Geoeffective interplanetary scale sizes derived from regression analysis of polar cap potentials, *J. Geophys. Res.*, *104*, 9989–9994.
- Codrescu, M. V., T. J. Fuller-Rowell, and J. C. Foster (1995), On the importance of E-field variability for Joule heating in the high-latitude thermosphere, *Geophys. Res. Lett.*, *22*, 2393–2396.
- Codrescu, M. V., T. J. Fuller-Rowell, J. C. Foster, J. M. Holt, and S. J. Cariglia (2000), Electric field variability associated with the Millstone Hill electric field model, *J. Geophys. Res.*, *105*, 5265–5273.
- Cowley, S. W. H. (1982), The causes of convection in the Earth's magnetosphere: A review of developments during the IMS, *Rev. Geophys.*, *20*, 531–565.
- Cowley, S. W. H., and M. Lockwood (1992), Excitation and decay of solar wind-driven flows in the magnetosphere-ionosphere system, *Ann. Geophys.*, *10*, 103–115.
- Crooker, N. U., G. L. Siscoe, C. T. Russell, and E. J. Smith (1982), Factors controlling degree of correlation between ISEE 1 and ISEE 3 interplanetary magnetic field measurements, *J. Geophys. Res.*, *87*, 2224–2230.
- Doyle, M. A., and W. J. Burke (1983), S3-2 measurements of the polar cap potential, *J. Geophys. Res.*, *88*, 9125–9133.
- Greenwald, R. A., et al. (1995), DARN/SuperDARN: A global view of high-latitude convection, *Space Sci. Rev.*, *71*, 763–796.
- Greenwald, R. A., J. M. Ruohoniemi, K. B. Baker, W. A. Bristow, G. J. Sofko, J.-P. Villain, M. Lester, and J. Slavin (1999), Convective response to a transient increase in dayside reconnection, *J. Geophys. Res.*, *104*, 10,007–10,015.
- Heppner, J. P. (1972), Polar-cap electric field distributions related to the interplanetary magnetic field direction, *J. Geophys. Res.*, *77*, 4877–4887.
- Lockwood, M., S. W. H. Cowley, and M. P. Freeman (1990), The excitation of plasma convection in the high-latitude ionosphere, *J. Geophys. Res.*, *95*, 7961–7972.
- Reiff, P. H., and J. G. Luhmann (1986), Solar wind control of the polar-cap voltage, in *Solar Wind-Magnetosphere Coupling*, edited by Y. Kamide and J. A. Slavin, pp. 453–476, Kluwer Acad., Norwell, Mass.
- Reiff, P. H., R. W. Spiro, R. A. Wolf, Y. Kamide, and J. H. King (1985), Comparison of polar cap potential drops estimated from solar wind and ground magnetometer data: CDAW 6, *J. Geophys. Res.*, *90*, 1318–1324.
- Rich, F. J., and M. Hairston (1994), Large-scale convection patterns observed by DMSP, *J. Geophys. Res.*, *99*, 3827–3844.
- Ruohoniemi, J. M., and K. B. Baker (1998), Large-scale imaging of high-latitude convection with Super Dual Auroral Radar Network HF radar observations, *J. Geophys. Res.*, *103*, 20,797–20,811.
- Ruohoniemi, J. M., and R. A. Greenwald (1998), The response of high-latitude convection to a sudden southward IMF turning, *Geophys. Res. Lett.*, *25*, 2913–2916.
- Shepherd, S. G., R. A. Greenwald, and J. M. Ruohoniemi (1999), A possible explanation for rapid, large-scale ionospheric responses to southward turnings of the IMF, *Geophys. Res. Lett.*, *26*, 3197–3200.

- Shepherd, S. G., J. M. Ruohoniemi, and R. A. Greenwald (2003), Testing the Hill model of transpolar potential with Super Dual Auroral Radar Network observations, *Geophys. Res. Lett.*, *30*(1), 1002, doi:10.1029/2002GL015426.
- Toffoletto, F. R., and T. W. Hill (1989), Mapping of the solar wind electric field to the Earth's polar caps, *J. Geophys. Res.*, *94*, 329–347.
- Weigel, R. S., A. J. Klimas, and D. Vassiliadis (2003), Solar wind coupling to and predictability of ground magnetic fields and their time derivatives, *J. Geophys. Res.*, *108*(A7), 1298, doi:10.1029/2002JA009627.
- Weimer, D. R. (2001), An improved model of ionospheric electric potentials including substorm perturbations and application to the Geospace Environment Modeling November 24, 1996, event, *J. Geophys. Res.*, *106*, 407–416.
-
- W. A. Bristow and J. M. Hughes, Geophysical Institute, University of Alaska Fairbanks, PO Box 757320, Fairbanks, AK 99775-7320, USA. (bill.bristow@gi.alaska.edu; hughesj@gi.alaska.edu)
- R. A. Greenwald, Applied Physics Laboratory, Johns Hopkins University, 11100 Johns Hopkins Road, Laurel, MD 20723-6099, USA. (ray.greenwald@jhuapl.edu)
- S. G. Shepherd, Thayer School of Engineering, Dartmouth College, 8000 Cummings Hall, Hanover, NH 03755, USA. (simon.shepherd@dartmouth.edu)